Journal of Applied Polymer Science

Effects of Copolymer Microstructure on the Properties of Electrospun Poly(L-lactide-co-ε-caprolactone) Absorbable Nerve Guide Tubes

Boontharika Thapsukhon,[1,2] Napaphat Thadavirul,[3] Pitt Supaphol,[3] Puttinan Meepowpan,[1,2] Robert Molloy,[1,4] Winita Punyodom[1,2,4]

[1]Department of Chemistry, Faculty of Science, Biomedical Polymers Technology Unit, Chiang Mai University, Chiang Mai 50200, Thailand

[2]Center of Excellence for Innovation in Chemistry, Department of Chemistry, Faculty of Science, Chiang Mai University, Chiang Mai 50200, Thailand

[3]The Petroleum and Petrochemical College, Chulalongkorn University, Soi Chulalongkorn 12, Pathumwan, Bangkok 10330, Thailand

[4]Materials Science Research Center, Faculty of Science, Chiang Mai University, Chiang Mai, 50200, Thailand

Correspondence to: W. Punyodom, (E-mail: winitacmu@gmail.com).

ABSTRACT: The main objective of this work has been to study the effects of copolymer microstructure, both chemical and physical, on the microporosity, *in vitro* hydrolytic degradability and biocompatibility of electrospun poly(L-lactide-*co*-ε-caprolactone), PLC, copolymer tubes for potential use as absorbable nerve guides. PLC copolymers with L : C compositions of 50 : 50 and 67 : 33 mol % were synthesized via the ring-opening copolymerization of L-lactide (L) and ε-caprolactone (C) at 120°C for 72 h using stannous octoate (tin(II) 2-ethylhexanoate) and *n*-hexanol as the initiating system. Electrospinning was carried out from solution in a dichloromethane/dimethylformamide (7 : 3 v/v) mixed solvent at room temperature. The *in vitro* hydrolytic degradation of the electrospun PLC tubes was studied in phosphate buffer saline over a period of 36 weeks. The microporous tubes were found to be gradually degradable by a simple hydrolysis mechanism leading to random chain scission. At the end of the degradation period, the % weight retentions of the PLC 50 : 50 and 67 : 33 tubes were 15.6% and 70.2%, respectively. Pore stability during storage as well as cell attachment and proliferation of mouse fibroblast cells (L929) showed the greater potential of the PLC 67 : 33 tubes for use as temporary scaffolds in reconstructive nerve surgery. © 2013 Wiley Periodicals, Inc. J. Appl. Polym. Sci. 130: 4357–4366, 2013

KEYWORDS: biodegradable; biocompatibility; biomedical applications; electrospinning; ring-opening polymerization

Received 11 February 2013; accepted 17 June 2013; Published online 20 July 2013
DOI: 10.1002/app.39675

INTRODUCTION

In peripheral nerve repair, end-to-end anastomosis is the preferred method for surgical intervention whenever tension-free suturing is possible. If not, then patients with loss of nerve tissue resulting in a nerve gap often require a nerve graft procedure.[1] However, autologous nerve grafts pose problems relating to donor site morbidity and neuroma formation.[2] Moreover, the functional recovery may not always be as required because of misdirection of the regenerating axons towards an inappropriate target.[3] Consequently, attempts have been made in recent years to produce absorbable nerve guides that bridge the nerve gap and provide a channel for the nerve ends to grow together.

A material that is to be used as an absorbable nerve guide needs to have, aside from biocompatibility and biodegradability, suitable porosity and mechanical characteristics.[4,5] Amongst the commercially available absorbable nerve guides that have been approved by the U.S. Food and Drug Administration (FDA) and Conformit European (CE) are Neurolac™ (poly(DL-lactide-*co*-ε-caprolactone)), Neurotube™ (poly(glycolic acid)), NeuraGen™ (Collagen Type I) and NeuroMatrix/Neuroflex™ (Collagen Type I).[6] The degradation rates of these tubes range from months (Neurotube™ in 3 months and NeuroMatrix™ in 7 months) to years (Neurolac™ in 16 months and NeuraGen™ in 4 years).[7] Synthetic polymers offer advantages over natural polymers in that they can be designed to give a wide range of properties. By careful control of their microstructure during both synthesis and processing, their various properties can be tailored for each particular case.

Nowadays, micro- or nanoporous scaffolds can be produced by three main methods, namely: phase separation,[8] self-assembly,[9]

and electrospinning.[10,11] Of these methods, electrospinning has become the most popular in recent years, generating a uniform and continuous mesh of fibers with diameters ranging from tens of nanometers to microns.[12,13] This technique uses static electricity to draw fibers from a polymer solution and deposit them on a surface. Electrospun membranes are highly porous and have very large surface-to-volume ratios. High porosity does not affect cell attachment but it does enhance cell proliferation due to the porous structure facilitating the transport of oxygen and nutrients. Recently, nanoscale scaffolds have been used for fabricating biomimetic frameworks in an attempt to mimic the nanostructure and hence the natural function of the extracellular matrix (ECM) in enhancing cell attachment, proliferation, and differentiation.[14] It has been noted that a suitable pore size and high porosity of the scaffold are necessary for cell ingrowth.[15]

Previous studies have shown that poly(L-lactide-*co*-ε-caprolactone) (PLC) scaffolds have good biocompatibility with many types of cells including smooth muscle cells, fibroblasts, osteoblasts, and cartilage-derived chondrocytes.[16–18] Synthetic aliphatic polyesters such as PLC undergo hydrolytic degradation when implanted into the human body.[19] During hydrolysis, water in the ECM attacks the ester linkages resulting in random chain scission of the acyl-oxygen (CO—O) bonds and a rapid decrease in the molecular weight of the polymer. This then leads to a loss of mass integrity (fragmentation), mass loss and removal of the hydrolysis products by the body's own biological processes.

The main objective of this present work has been to study the effects of the physico-chemical microstructure of electrospun PLC copolymer tubes on their microporosity, *in vitro* hydrolytic degradability and biological interaction with mouse fibroblast cells (L929). Although PLC copolymers are relatively well known as far as their use in biomedical applications is concerned, the effects of their microstructural variations (copolymer composition, monomer sequencing, matrix morphology, etc.) on their suitability for a particular application are rarely discussed in detail. These variations arise from differences and/or inconsistencies in the synthesis and processing conditions used and often result in an unacceptably wide variation in properties. This article aims to contribute to our understanding of this microstructure-property relationship and at the same time highlight the critical importance of microstructural control in the synthesis and fabrication of an absorbable nerve guide.

EXPERIMENTAL

Materials

L-Lactide was synthesized from L-lactic acid (Carlo Erba, 88%) and purified by recrystallization from ethyl acetate to at least 99.9% purity as determined by DSC Purity Analysis. ε-Caprolactone (Acros, 99%) and stannous octoate ($Sn(Oct)_2$, Sigma-Aldrich, 95%) were purified by vacuum distillation and *n*-hexanol (Sigma-Aldrich, 98%) by normal distillation. Dichloromethane (DCM), dimethylformamide (DMF), chloroform, and methanol (all AR grade, LabScan) were used as received. The molecular structures of the L-lactide and ε-caprolactone comonomers are shown in Figure 1.

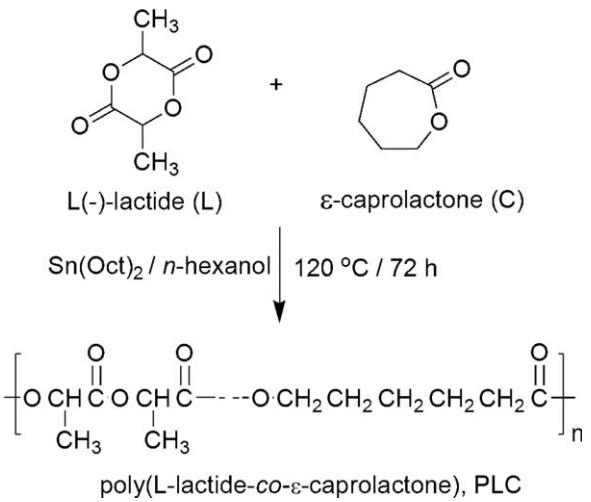

Figure 1. Synthesis of the poly(L-lactide-*co*-ε-caprolactone), PLC, copolymers.

Synthesis and Characterization of Poly (L-lactide-co-ε-caprolactone)

PLC copolymers of L : C = 50 : 50 and 67 : 33 mol % compositions (hereafter referred to as PLC 50 : 50 and PLC 67 : 33) were synthesized by ring-opening polymerization (ROP) in bulk at 120°C for 72 h using $Sn(Oct)_2$ 0.1 mol % and *n*-hexanol 0.01 mol % as the initiating system, as shown in Figure 1. The copolymers were purified by dissolution in chloroform, precipitation in cold methanol, and vacuum drying at 40°C for 48 h. The copolymer compositions were determined from their ^{1}H-NMR spectra and their monomer sequencing from their ^{13}C-NMR spectra, as recorded on a Bruker Avance DPX-400 NMR Spectrometer. The number-average and weight-average molecular weights ($\overline{M}_n$ and $\overline{M}_w$) and polydispersities ($\overline{M}_w/\overline{M}_n$) of the copolymers were determined by gel permeation chromatography (GPC) using a Waters 717 Autosampler GPC employing universal calibration with narrow molecular weight polystyrene standards and dual refractive index and viscosity detectors. Tetrahydrofuran (THF) was used as the solvent at a flow rate of 1.0 ml min^{-1} at 40°C with a sample solution concentration of 3% (w/v) and an injection volume of 100 μL. Intrinsic viscosity, [η], was determined by dilute-solution viscometry using chloroform as the solvent at 25°C. Differential scanning calorimetry (DSC) measurements were carried out on a Perkin-Elmer DSC7 over the temperature range of −10 to 200°C and at a heating rate of 10°C min^{-1}.

Nerve Guide Tube and Flat Membrane Preparation by Electrospinning

For nerve guide tube and flat membrane preparation, the PLC 50 : 50 and PLC 67 : 33 copolymers were dissolved in a mixed solvent of DCM:DMF = 7 : 3 (v/v) to give polymer solutions of varying concentrations from 8 to 14% (w/v). For the process of electrospinning, the polymer solution was placed in a 5 mL glass syringe fitted with a stainless steel blunt-ended needle (20-gauge, outer diameter 0.91 mm). PLC microfibers were electrospun at applied voltages in the range of 10–20 kV using a Gamma High Voltage Research DC Power Supply. A grounded collection plate of aluminum foil was located at a fixed distance

Table I. Characterization of the Poly(L-lactide-*co*-ε-caprolactone), PLC, Copolymers

Comonomer feed ratio[a]	Copolymer composition[a]	Molecular weight		Intrinsic viscosity[b]			Conversion[e]
L : C	L : C	$\overline{M}_n$	$\overline{M}_w/\overline{M}_n$	(dL g^{-1})	T_g[c] (°C)	T_m[d] (°C)	(%)
50 : 50	49.9 : 50.1	1.4×10^4	3.2	1.62	−10	-	96
67 : 33	66.7 : 33.3	1.7×10^4	3.1	1.66	23	150	97

[a] In mol %; [b]Measured in $CHCl_3$ at 25°C; [c]Mid-point; [d]Peak maximum. [e]After purification.

of 15 cm from the needle tip to give flat membranes for biocompatibility testing and structure determination. For tubes, a grounded rotating (300 rpm) mandrel in the form of a Kirchner-wire rod (1.2 mm in diameter) was used as the target to collect the microfibers for the *in vitro* hydrolytic degradation study. As-spun tubes and membranes were dried under vacuum at room temperature overnight. Their microporous surface topographies were observed using a JEOL 5910 LV scanning electron microscope (SEM) at an acceleration voltage of 15 kV. Multiple SEM images of 50 fibers were analyzed by NIH ImageJ software to determine the average fiber diameters.[15,20]

In Vitro Hydrolytic Degradation Studies

The electrospun PLC 50 : 50 and 67 : 33 tubes were cut into 15 mm lengths for *in vitro* hydrolytic degradation studies. Preweighed tubes were placed into screw-top glass bottles containing phosphate buffer saline (PBS, pH 7.40 ± 0.01) with a weight-to-volume ratio of 1.4×10^{-3} g mL^{-1} and incubated at a temperature of 37.0 ± 0.1°C for 36 weeks. At designated time intervals throughout the 36-week period, bottles were removed from the incubator and the electrospun tubes filtered off, washed carefully with deionized water, dried in a vacuum oven at room temperature to constant weight and weighed. The pH of the PBS was also measured. Reductions in both PLC weight and molecular weight were determined as a function of time. The % weight loss was calculated from eq. (1):

$$\%\ \text{Weight loss} = \frac{w_0 - w_t}{w_0} \times 100\% \quad (1)$$

where w_0 = initial weight and w_t = weight at time t.

Biocompatibility

Cell Culture. Mouse fibroblast cells (L929) were cultured as a monolayer in 10% serum-containing Dulbecco's Modified

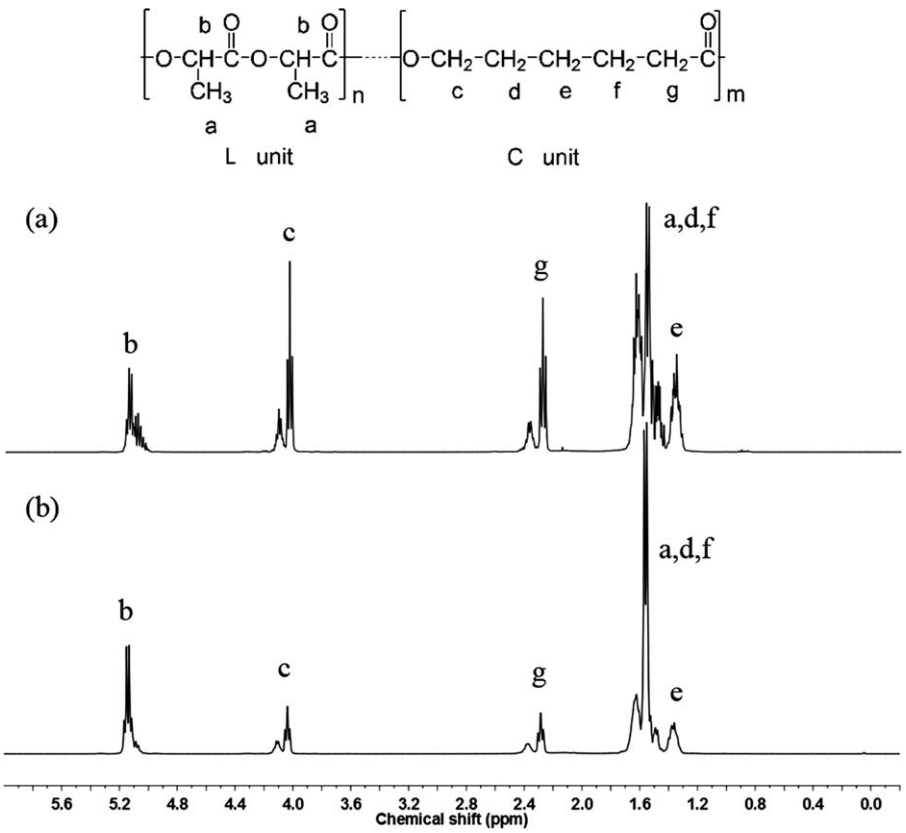

Figure 2. 400 MHz ^{1}H-NMR spectra of the PLC copolymers recorded in $CDCl_3$ as solvent at room temperature: (a) PLC 50 : 50 and (b) PLC 67 : 33. (Proton assignments as shown).

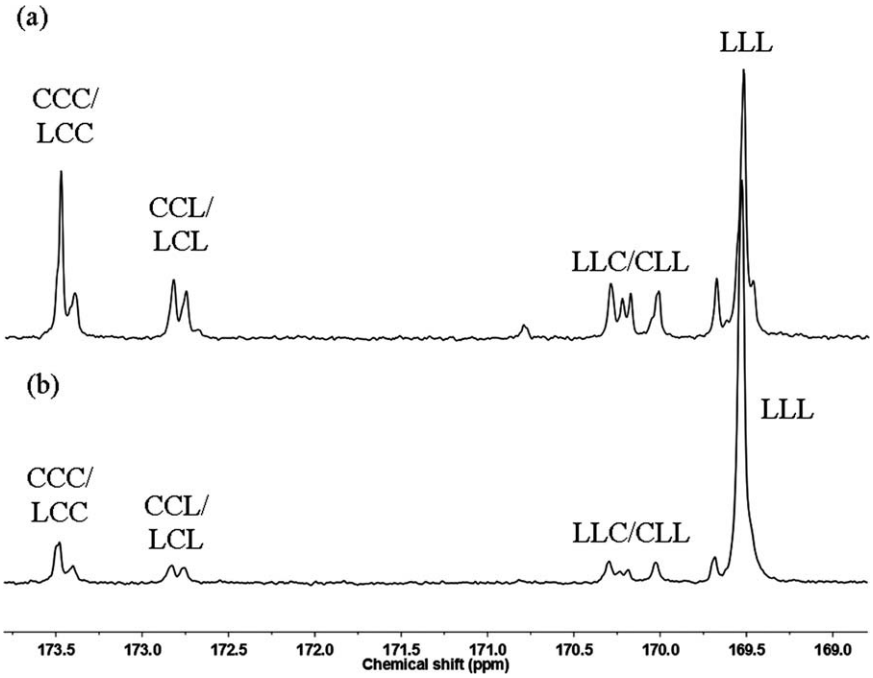

Figure 3. Expanded carbonyl carbon regions of the 100 MHz ^{13}C-NMR spectra of the PLC copolymers recorded in $CDCl_3$ as solvent at room temperature: (a) PLC 50 : 50 and (b) PLC 67 : 33. (Triad assignments as shown).

Eagle's Medium (DMEM, Sigma-Aldrich) supplemented with 10% fetal bovine serum (FBS, Biochrom AG), 1% L-glutamine (Invitrogen) and a 1% antibiotic and antimycotic formulation containing penicillin G sodium, streptomycin sulfate, and amphotericin B (Invitrogen). The medium was replaced every 2 days and the cultures maintained at 37.0 ± 0.1°C in a humidified atmosphere containing 5% CO_2.

Cell Seeding. Prior to seeding of the L929 cells, each of the electrospun PLC 50 : 50 and 67 : 33 membranes was cut into circular discs (15 mm in diameter). Each specimen was placed in the well of a 24-well tissue-culture polystyrene plate and sterilized in 70% ethanol for 30 min. The specimens were washed with autoclaved deionized water, PBS and subsequently immersed in DMEM overnight. To ensure close contact between the specimens and the wells, the specimens were pressed with a metal ring (12 mm in diameter). The cultured L929 cells were trypsinized in 0.25% trypsin containing 1 m*M* ethylenediamine tetraacetic acid (EDTA) and counted by a hemacytometer (Hausser Scientific). For cell attachment, L929 cells were seeded at a density of 6×10^4 cells cm^{-2} on the specimens and allowed to attach for 2, 4, and 6 h. For cell proliferation, the L929 cells were seeded at a density of 3×10^4 cells cm^{-2} and allowed to attach for 24, 48, and 72 h. A cover glass was used as the control.

Cell Morphology. After the removal of the culture medium, the specimens were rinsed with PBS twice and then fixed with 3% glutaraldehyde solution for 30 min at room temperature, dehydrated through a series of graded alcohol solutions (30, 50, 70, 90, and 100%), dried in 100% hexamethyldisilazane (HMDS, Sigma) for 5 min and finally air-dried overnight. Dry specimens were sputter-coated with gold for SEM microscopic analysis of the cell morphology at an accelerating voltage of 15 kV.

RESULTS AND DISCUSSION

PLC Copolymer Characterization

The L : C comonomer feeds and the final % conversions and characteristic properties of the PLC copolymers are summarized in Table I. Copolymer compositions (L : C, mol %) were determined from the ^{1}H-NMR spectra in Figure 2 by ratioing the peak area integrations corresponding to the L-methine protons at δ 5.1–5.2 ppm and the C ε-methylene protons at δ 4.0–4.2 ppm. It was found that the copolymer compositions, which are average values over a compositional distribution, were almost equivalent (±1%) to the initial comonomer feeds. This is consistent with their near-quantitative (≥96%) conversions.

Monomer sequencing in the copolymers was characterized by ^{13}C-NMR, specifically from the expanded carbonyl carbon (C═O) region of the spectrum from δ 169–174 ppm. The various peaks in this region can be assigned to the C═O carbons of the middle units of various triad sequences, as labeled in Figure 3. The appearance of mixed triad peaks in between the CCC peak at 173.5 ppm and the LLL peak at 169.5 ppm confirms that the monomer sequencing was randomized to a limited extent. However, it is more accurate to describe the copolymers as being of the statistical (gradient) type, i.e., having an architecture somewhere in between a completely random and a block copolymer. This is due to the much different monomer reactivity (L > C) ratios.[21] This monomer sequencing is unique not only to the comonomer pairing but also to the synthesis conditions employed and, even at the same composition, can have a significant effect on copolymer properties.

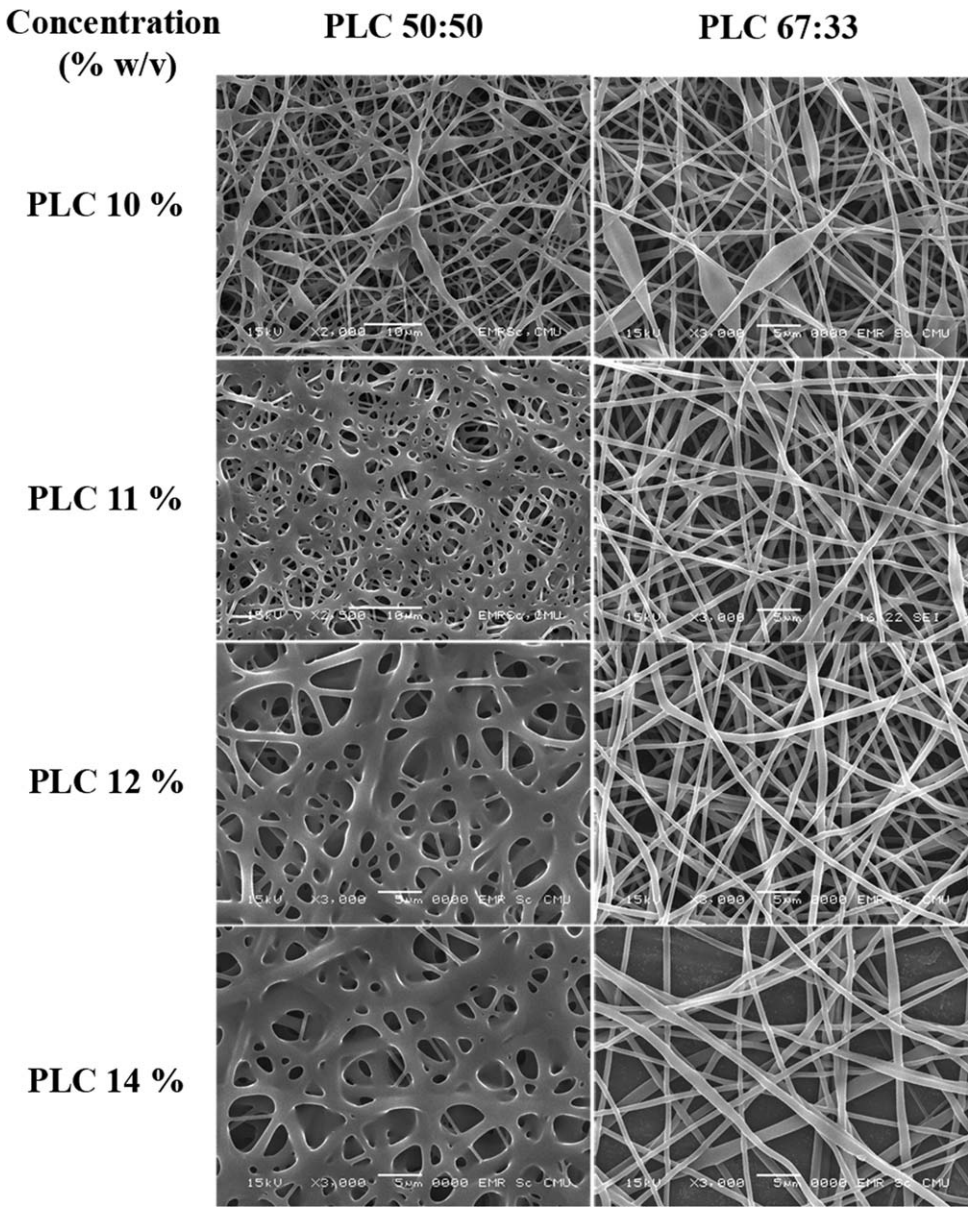

Figure 4. SEM images of PLC 50 : 50 and PLC 67 : 33 microfibers electrospun at an applied voltage of 15 kV from different solution concentrations of 10%, 11%, 12%, and 14% w/v. (Magnification: ×3000).

Effects of Electrospinning Conditions

Copolymer Solution Concentration. It was observed by SEM that PLC 50 : 50 and 67 : 33 copolymer solutions, which were lower than 11% (w/v) in concentration tended to give rise to bead formation in the electrospun fibers. The most suitable concentration range to give bead-free, well-defined microfiber meshes was 11–14% (w/v). SEM images of the PLC 50 : 50 and 67 : 33 electrospun fibers from different solution concentrations at a constant applied voltage of 15 kV are shown in Figure 4, while the relationship between the average fiber diameter and solution concentration is shown in Figure 5. As expected, the fiber diameter decreased with decreasing concentration with the lower limit determined by bead formation. When comparing the two compositions in Figure 4, the apparent merging of the PLC 50 : 50 fibers is attributed to their lower glass transition

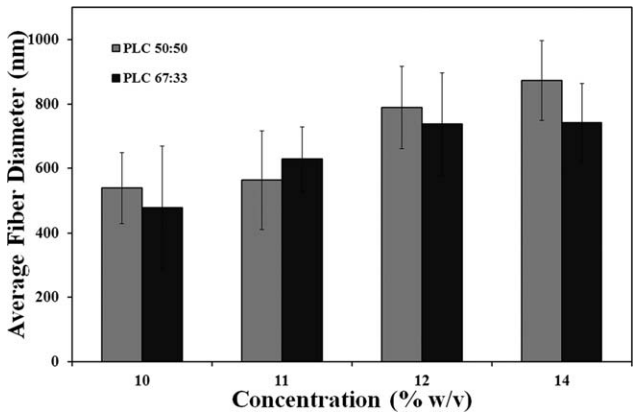

Figure 5. Relationship between average fiber diameter and copolymer solution concentration at an applied voltage of 15 kV.

Applied Polymer SCIENCE

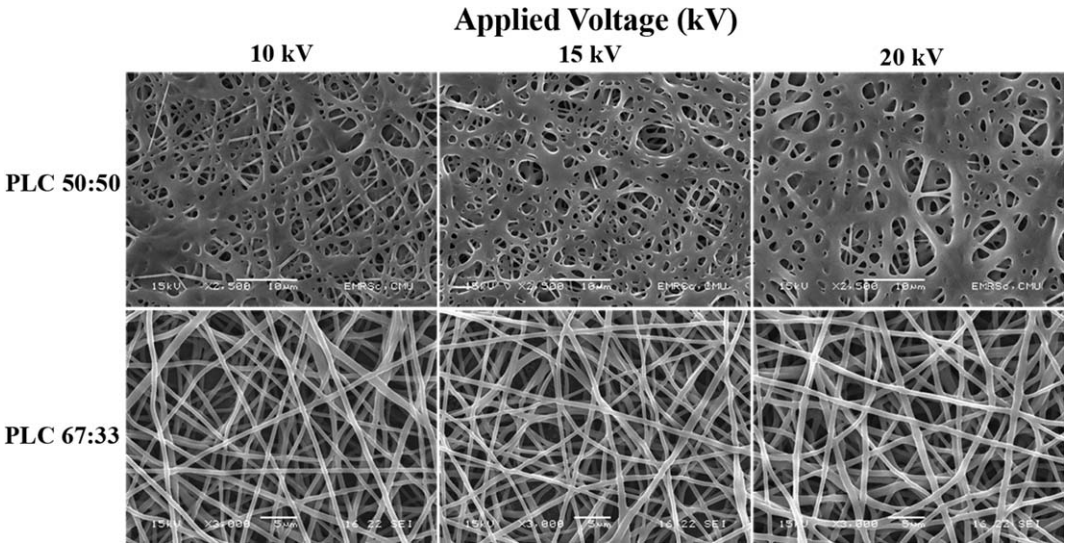

Figure 6. SEM images of PLC 50 : 50 and PLC 67 : 33 microfibers electrospun from a constant solution concentration of 11% (w/v) at different applied voltages of 10, 15, and 20 kV. (Magnification: ×2500 for PLC50 : 50 and ×3000 for PLC 67 : 33).

temperature T_g and lack of crystallinity. This is discussed in more detail in the following section on pore stability.

Applied Voltage. SEM images of the PLC microfibers electrospun at different applied voltages at the same solution concentration of 11% (w/v) are shown in Figure 6. The fiber diameter tended to decrease with increasing applied voltage although the effect was not as pronounced as that of decreasing solution concentration. Increasing the applied voltage increases the electrostatic stress on the emerging jet, which in turn increases the amount of draw on the fiber as it is formed, thereby decreasing the diameter. The variation in fiber diameter with the applied voltage is shown in Figure 7. However, it should be emphasized that the observed effect of the applied voltage, as with the solution concentration previously, is specific for a particular polymer/solvent combination and set of electrospinning conditions.

Pore Stability

Since, the main purpose of this work has been to produce electrospun tubes suitable for use as nerve guides, the tubes should be able to maintain their shape (i.e., be dimensionally stable) for at least 2–3 months after nerve repair. In addition, they need to be stable during storage for potentially long periods at room temperature before use. In this study, electrospun PLC 50 : 50 and PLC 67 : 33 membranes were stored in vacuum desiccators for 14 weeks and changes in their pore structure followed by SEM. As shown in Figure 8, whereas the interconnecting pore structure of the PLC 50 : 50 copolymer gradually merged together after 14 weeks [Figure 8(a,c)], the pore structure of the PLC 67 : 33 copolymer remained stable during this period [Figure 8(b,d)]. These results suggest that storage stability at room temperature depends on the copolymer having (a) a high enough glass transition temperature, T_g, and preferably (b) partial crystallinity in order to stiffen the copolymer matrix. Each of these properties helps to restrict molecular motion at the microscopic level and therefore pore merging at the macroscopic level. Thus, the pore structure of the PLC 50 : 50 copolymer with its low T_g of -10°C combined with its amorphous matrix morphology (from DSC analysis) was found to be much less stable when stored at ambient temperature than the PLC 67 : 33 copolymer with its higher T_g of 23°C and its semicrystalline morphology (DSC melting point T_m (peak) $\approx$ 150°C).

Tube Dimensions and Porosity

The electrospun PLC 50 : 50 and 67 : 33 tubes, as prepared, were 10 cm in length and 1.2 mm in inner diameter, as determined microscopically. The photographs and SEM images are shown in Figure 9(a–c). The interconnecting internal pore structure of the tubes is shown in the cross-sectional image in Figure 9(d). On the macroscopic scale, the tubes appeared white, opaque and were both flexible and slightly elastic in nature. The data in Table II compares their average fiber diameters, pore sizes, wall thicknesses, and % porosities, as obtained under what were considered to be optimum conditions. The PLC 67 : 33 copolymer tended to give larger fiber diameters and pore sizes, which also helped to enhance its pore stability.

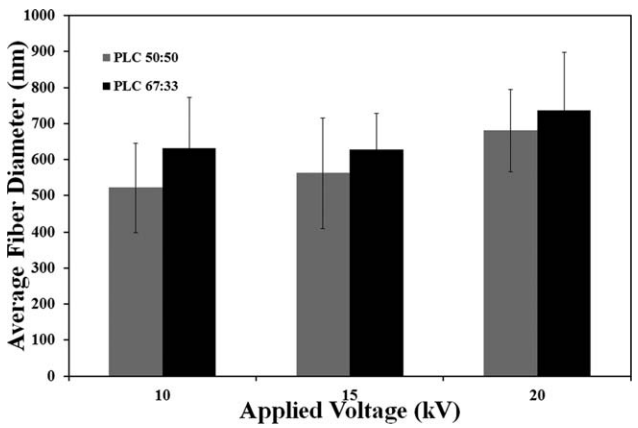

Figure 7. Relationship between fiber diameter and applied voltage for the PLC 50 : 50 and PLC 67 : 33 microfibers at a constant solution concentration of 11% (w/v).

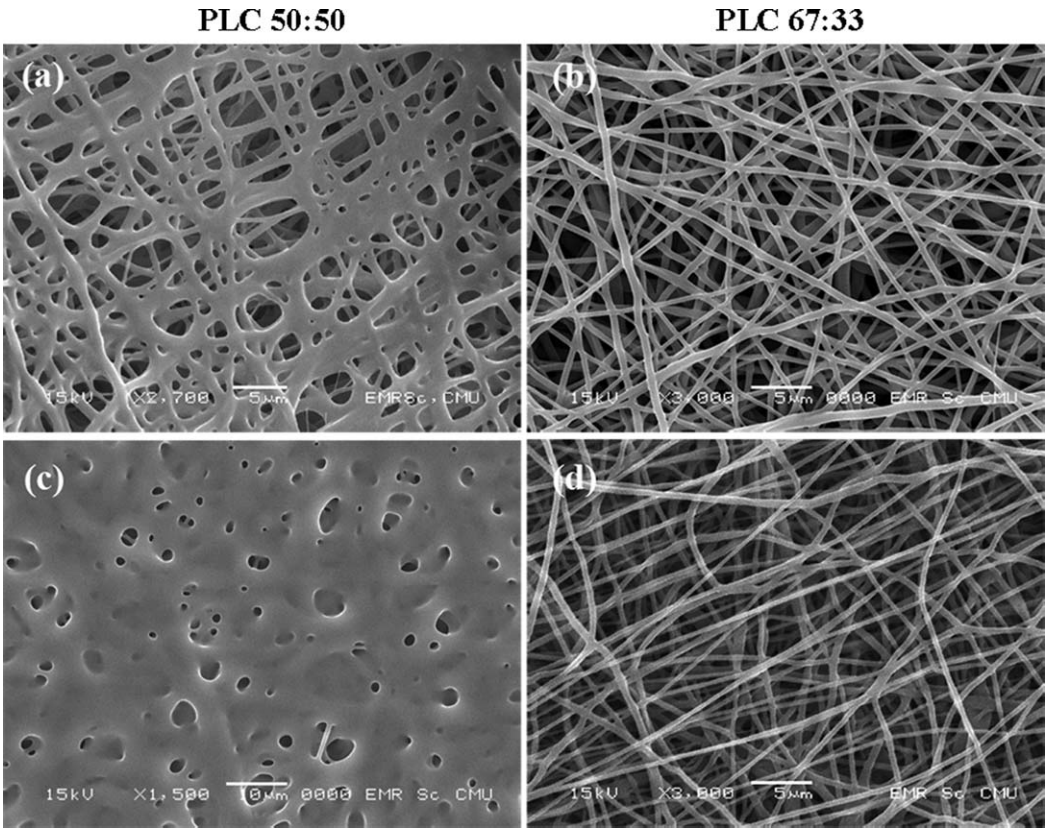

Figure 8. SEM images of the PLC 50 : 50 and PLC 67 : 33 membranes: (a–b) after initial preparation and (c–d) after storage for 14 weeks.

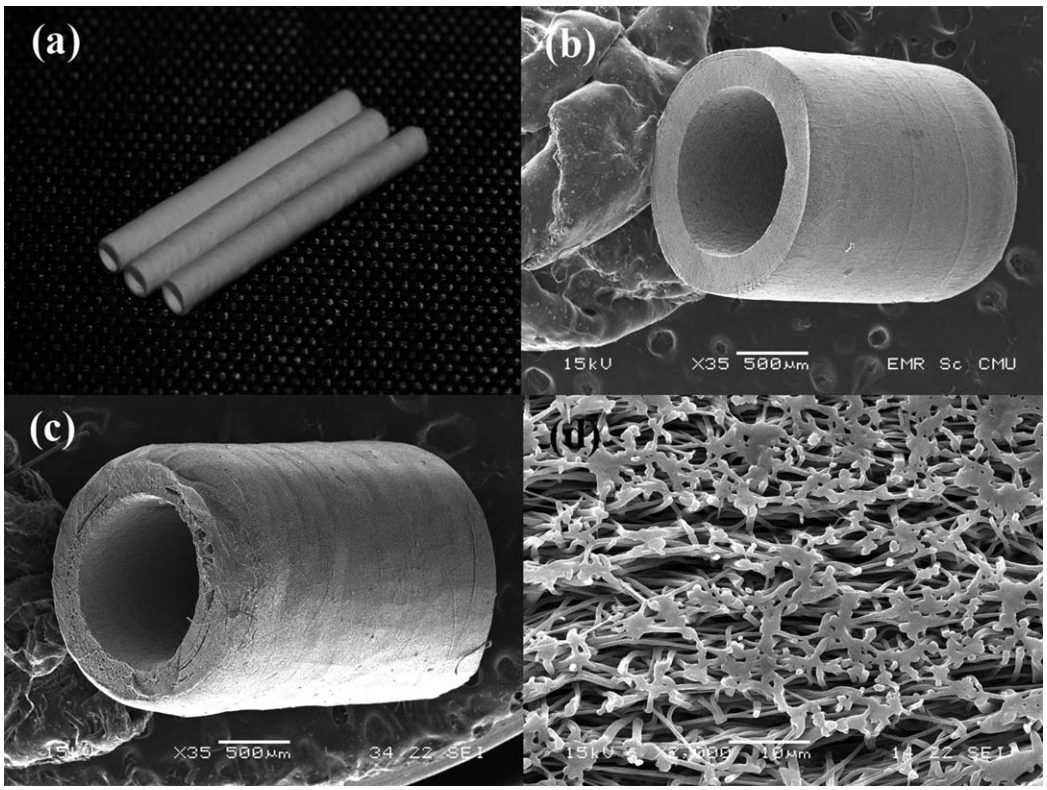

Figure 9. (a) Photographs and (b–d) SEM images of PLC copolymer tubes: (b) PLC 50 : 50 tube, (c) PLC 67 : 33 tube, and (d) cross-section of PLC 67 : 33 tube.

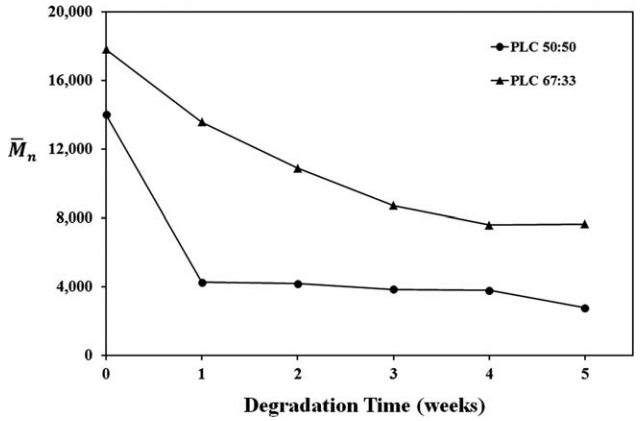

Figure 10. Number-average molecular weight changes for the PLC 50 : 50 and PLC 67 : 33 tubes during *in vitro* hydrolysis.

In Vitro Hydrolytic Degradation

Molecular Weight Reduction. The decreases in $\overline{M}_n$ of both copolymers with degradation time are compared in Figure 10. The fast initial decreases are typical of a random chain scission mechanism. Interestingly, despite the fact that caprolactone (C) units are more hydrophobic than L-lactide (L) units and therefore hydrolyse more slowly, the rate of decrease of $\overline{M}_n$ of the PLC 50 : 50 tubes was faster than that of the PLC 67 : 33 tubes. This was due to the fact that PLC 50 : 50 was completely amorphous whereas PLC 67 : 33 was semicrystalline. Hydrolysis occurs preferentially in the amorphous regions of the matrix where the chains are more loosely packed than in the highly ordered crystalline regions. Therefore, despite its lower C content, PLC 67 : 33 hydrolyzed more slowly since its semicrystalline matrix contained proportionately less free volume through which diffusing water molecules could access the hydrolysable ester bonds.

Weight Loss and pH Changes. The weight loss changes for the PLC 50 : 50 and 67 : 33 tubes together with the changes in pH of the PBS immersion medium are shown in Figure 11. Both compositions exhibited a slow initial weight loss over the first 6–8 weeks, accelerating during the later stages as the decrease in molecular weight eventually led to a loss of mass integrity and fragmentation. The PLC 50 : 50 tubes degraded faster due to their amorphous nature with a weight loss of 85% after 36 weeks. In contrast, the weight loss of the PLC 67 : 33 tubes over the same time period was only about 30%.

Since PLC is a relatively hydrophobic material, degradation proceeds via surface rather than bulk erosion. Eventually, this surface erosion combined with the ongoing molecular weight decrease causes micro defects to occur, which then facilitates the ingress of water molecules into the bulk interior of the copolymer matrix, thereby accelerating the degradation. At the same

Table II. Dimensions and Porosities of the Electrospun PLC Copolymer Tubes

Copolymer	Average fiber diameter (nm)	Average wall thickness (μm)	Average pore size (nm)	Porosity (%)
PLC 50 : 50[a]	558 ± 181	450 ± 50	237 ± 35	85
PLC 67 : 33[b]	808 ± 254	485 ± 35	660 ± 23	89

Values calculated from SEM images using ImageJ software. Electrospinning conditions:
[a] 12% (w/v) solution concentration at 15 kV; [b] 11% (w/v) solution concentration at 15 kV.

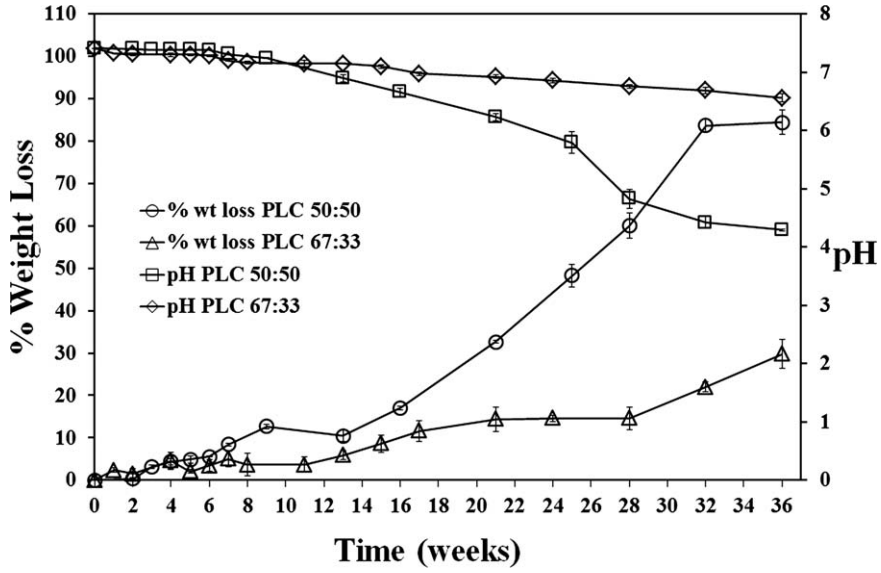

Figure 11. Weight loss and pH decreases for the PLC 50 : 50 and PLC 67 : 33 tubes during *in vitro* hydrolytic degradation.

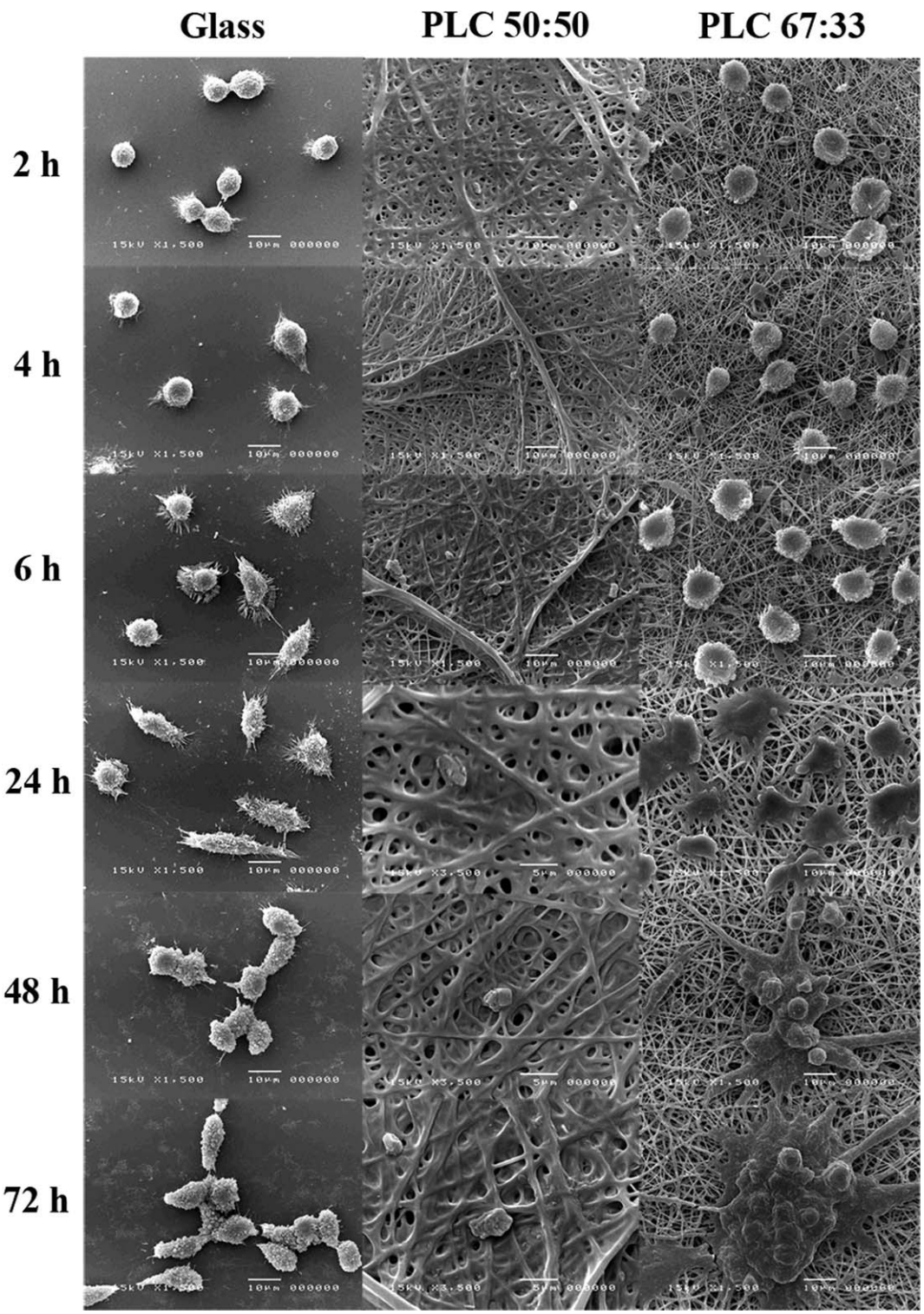

Figure 12. SEM images of L929 cultured cells on the PLC 50 : 50 and PLC 67 : 33 membrane surfaces after 2, 4, 6, 24, 48, and 72 h seeding. (Magnification: ×1500).

time, the decreasing pH of the PBS solution, resulting from the release of acidic hydrolysis products, also contributes towards accelerating the degradation by acid-catalysis of the ester hydrolysis mechanism. The correspondence between the weight loss and pH changes is clearly evident in Figure 11.

Cell Attachment and Proliferation

The SEM images of L929 cultured cells on the PLC membranes after 2, 4, 6, 12, 24, and 72 h seeding are shown in Figure 12. The PLC 67 : 33 surface exhibited rounded healthy cells from 2 to 6 h, which then became elongated and well spread after 48

to 72 h, similar to those on the cover glass control. The number of cells on both the PLC 67 : 33 surface and on the cover glass increased with incubation time. In comparison, cell attachment and proliferation were significantly less on the PLC 50 : 50 surface, which was probably because of a combination of factors such as its greater hydrophobicity (higher C content), merged pore structure, and its faster hydrolytic degradation leading to the release of acidic products.

CONCLUSIONS

In conclusion, this research has set out to study the effects of copolymer microstructure on the properties of electrospun PLC absorbable nerve guide tubes. Apart from biodegradability (hydrolysability) and biocompatibility, microporosity is also important in a nerve guide tube because it allows for cell infiltration as well as fluid and nutrient diffusion from the surrounding tissue to the lumen of the tube. As the results here have shown, every aspect of both chemical and physical microstructure needs to be controlled if predictable and reproducible properties are to be obtained. This is because the microstructure obtained is unique to the synthesis and processing conditions employed. From synthesis, statistical (gradient) PLC copolymers were obtained due to the differing monomer reactivity ratios. Whereas the 50 : 50 copolymer was amorphous with a subambient T_g of −10°C, the 67 : 33 copolymer was semicrystalline with a near-ambient T_g of 23°C resulting in a more stable pore structure when stored at room temperature. However, pore stability was also dependent on the fiber diameter and pore size, properties which were determined by the processing conditions. Thus, it is only by bringing all of this information together and by understanding the microstructure-property relationships involved that we can effectively design, synthesize, and fabricate a PLC copolymer for such a specialist application as this where the property requirements are so stringent. Taking into account all of the results presented here, it can be concluded that PLC shows considerable potential for use as an electrospun absorbable nerve guide material provided that the L content is high enough to ensure pore stability. The 67 : 33 composition is a suitable starting point.

ACKNOWLEDGMENTS

This research was supported by a scholarship (to B.T.) under the Strategic Scholarships for Frontier Research Network for a PhD Program from Thailand's Commission on Higher Education (CHE). Additional financial support under the CHE's National Research University Project as well as from the National Metal and Materials Technology Center (MTEC), the Center for Innovation in Chemistry (PERCH-CIC) and the Graduate School of Chiang Mai University is also gratefully acknowledged.

REFERENCES

1. Lundorg, G. R.; Rorn, B.; Dahlin, L.; Danielsen, N.; Holmberg, J. *J. Hand. Surg.* **1997**, *22*, 99.
2. Dellon, A. L.; Mackinnon, S. E. *Plast. Reconstr. Surg.* **1988**, *82*, 849.
3. Jiang, X.; Lim, S. H.; Mao, H.-Q.; Chew, S. Y. *Exp. Neurol.* **2010**, *223*, 86.
4. Luis, A. L.; Rodrigues, J. M.; Lobato, J. V.; Lopes, M. A.; Amado, S.; Veloso, A. P.; Armada-da-Siva, P. A. S.; Raimando, S.; Geuna S.; Ferreira, A. J.; Varejão, A. S. P.; Santos, J. D.; Maurício, A. C. *Biomed. Mater. Eng.* **2007**, *17*, 39.
5. Liao, S.; Chan, C. K.; Ramakrishna, S. *Mater. Sci. Eng. C: Mater.* **2008**, *28*, 1189.
6. Meek, M. F.; Coert, J. H. *Ann. Plast. Surg.* **2008**, *60*, 466.
7. Schlosshauer, B.; Dreesmann, L.; Schaller, H. E.; Sinis, N. *Neurosurgery* **2006**, *59*, 740.
8. Yang, F.; Murugan, R.; Ramakrishna, S.; Wang, X.; Ma, Y. X.; Wang, S. *Biomaterials* **2004**, *25*, 1891.
9. Jun, H. W.; Yuwono, V.; Paramonov, S. E.; Hartgerink, J. D. *Adv. Mater.* **2005**, *17*, 2612.
10. Ramakrishna, S.; Fujihara, K.; Teo, W. E.; Lim, T. C.; Ma, Z. An Introduction to Electrospinning and Nanofibers; World Scientific: Singapore, **2005**; p 40.
11. Karami, Z.; Rezaeian, I.; Zahedi, P.; Abdollahi, M. *J. Appl. Polym. Sci.* **2012**, *129*, 756.
12. Murugan R.; Ramakrishna, S. *Tissue Eng.* **2006**, *12*, 435.
13. Rutledge, G. C.; Fridrikh, S. V. *Adv. Drug Deliv. Rev.* **2007**, *59*, 1384.
14. Liao, G.-Y.; Chen, L.; Zeng, X.-Y.; Zhou, X.-P.; Xie, X.-L.; Peng, E. J.; Ye, Z.-Q.; Mai, Y.-W. *J. Appl. Polym. Sci.* **2010**, *120*, 2154.
15. Semnani, D.; Ghasemi-Mobarakeh, L.; Morshed, M.; Nasr-Esfahani, M.-H. *J. Appl. Polym. Sci.* **2009**, *111*, 317.
16. Amass, W.; Amass, A.; Tighe, B. J. *Polym. Int.* **1998**, *47*, 89.
17. Sun, M.; Kingham, P. J.; Reid, A. J.; Armstrong, S. J.; Terenghi, G.; Downes, S. *J. Biomed. Mater. Res. A* **2010**, *93*, 1470.
18. Xiaoqiang, L.; Yan, S.; Rui, C.; Chuanglong, H.; Hongsheng, W.; Xiumei, M. *J. Appl. Polym. Sci.* **2009**, *111*, 1564.
19. Liu, C.; Xia, Z.; Czernuszka, J. T. *Chem. Eng. Res. Des.* **2007**, *85*, 1051.
20. Abramoff, M. D.; Magalhaes, P. J.; Ram, S. J. *Biophotonics Inter.* **2004**, *11*, 36.
21. Kricheldorf, H. R.; Berl, M.; Scharnagl, N. *Macromolecules* **1988**, *21*, 286.